Materials Science & Engineering A 715 (2018) 25–32

Contents lists available at ScienceDirect

Materials Science & Engineering A

journal homepage: www.elsevier.com/locate/msea

Control of inter/intra-granular κ-carbides and its influence on overall mechanical properties of a Fe-11Mn-10Al-1.25C low density steel

Degang Liu, Minghui Cai*, Hua Ding*, Dong Han

School of Materials Science & Engineering, Northeastern University, Shenyang 110819, China

ARTICLE INFO

Keywords:
Medium Mn low density steel
Inter/intra-granular κ-carbides
Microstructural evolution
Tensile properties
Planar glide

ABSTRACT

In this study, a novel ultra-high yield strength Fe-11Mn-10Al-1.25C low density steel was developed with aiming to fundamentally understand the formation of inter/intra-granular κ-carbides and its influence on the overall mechanical properties by varying cooling patterns, e.g. air cooling (AC), water quenching (WQ) and intensive quenching (IQ). The results show that the IQ microstructure is almost fully austenitic with very fine intra-granular κ-carbides of less than 13 nm, which is totally different from the chain-like ferrite and coarse inter-granular κ-carbides of 0.6–2.6 μm in both cases of AC and WQ. In contrast, the IQ sample exhibits similar high YS and UTS values (~ 1.1 GPa) to the others but significantly an enhanced ductility of ~ 29.3%, revealing an excellent balance of strength and ductility, i.e. the product of strength and ductility (PSE) can reach as high as 32.1 GPa%. The improved overall performance and continuously increasing strain hardening are dominated by planar glide, which is mainly attributed to the uniform distribution of nano-sized and shearable κ-carbides in the austenitic matrix. These results may provide theoretical supports for the κ-carbides-related alloy design and microstructural modification of ultra-high-strength medium Mn low density steels.

1. Introduction

With the focus on reducing the car weight and further limiting the amount of exhaust emissions, automakers have been devoting to manufacturing the lighter and safer vehicles. As a solution, the application of low density steels (also called high Al steels) has been proposed as an efficient approach to realize the automotive lightweight in comparison with the conventional transformation/twinning-induced plasticity (TRIP/TWIP) steels [1,2]. Therefore, developing low density steels has aroused much attention in recent years, owing to the desirable strength to density ratio and the ease with which it can be formed into the complex thin-walled components.

Low density steels have been designed with considerable Al addition (e.g. ~ 10%) obtaining density reductions of 10–13% or even higher [3]. A typical microstructure of low density steels may involve the austenite (γ), ferrite (α) or κ-carbide, depending on alloy compositions [3–11]. For the commonly used Fe-Mn-Al-C quaternary alloy system, C and Mn are the austenitic stabilizing elements, while Al is a strong ferrite forming element [11]. The addition of Al can raise the solvus of both inter/intra-granular κ-carbides [12]. Thus, the κ-carbides with an ordered face-centered cubic (fcc) $L'1_2$ type easily form inside the austenite by spinodal decomposition during quenching [3,13]. The space group of $L'1_2$ structure is Pm3m, with Fe or Mn atoms occupying the face-centered positions, Al atoms occupying the cornered positions and C atoms occupying the body-centered positions [11]. Meanwhile, the decomposition of austenite to ferrite and κ-carbide occurs by the eutectoid reaction during annealing or isothermal aging [8–11]. The difference in phase constituents and the size, morphology and distribution of κ-carbides eventually influence the resulting mechanical properties and deformation behavior of low density steels.

Frommeyer et al. [3] first reported the high strength and ductile Fe-(18-28)Mn-(10-12)Al-(1.0-1.2)C (wt%) triplex steels, in which the matrix is austenitic with some amount of ferrite (~ 7%) and nano-sized κ-carbides. Ding et al. [5] demonstrated that the fully austenitic structure with the dispersed nano-sized κ-carbides exhibits high tensile ductility in Fe-18Mn-10Al-1.2C steels. Recently, low density steels with less Mn addition have attracted more attention to reduce the cost of production. For example, a triplex Fe-12Mn-8Al-0.8C steel was proposed in our preliminary work to achieve a superior combination of high strength, over 900 MPa and good ductility, ~ 46% [7]. The addition of Cu has been proposed to further improve the yield strength of a novel ultra-high-strength duplex lightweight Fe-12Mn-7Al-0.5C-3Cu steel [9]. In addition, the formation of κ-carbides has been extensively investigated in low density steels [8–11,13,14]. A few studies demonstrate that the coarse κ-carbide particles distributed along grain boundaries dramatically deteriorated the ductility of low density steels

* Corresponding authors.
E-mail addresses: cmhing@126.com (M. Cai), hding@263.net (H. Ding).

https://doi.org/10.1016/j.msea.2017.12.102
Received 4 August 2017; Received in revised form 14 December 2017; Accepted 28 December 2017
Available online 29 December 2017

due to the easier stress concentration at interfaces [10,11,14]. Thus, it is critical to control the size, fraction and distribution of such κ-carbides to improve the overall performance of medium Mn low density steels. However, no systematic studies on how to control the inter/intra-granular κ-carbides in the 3rd-generation lightweight automotive steels have been reported yet so far.

Therefore, the present work aims to develop a novel medium Mn low density steel with a composition of Fe-11Mn-10Al-1.25C. Accordingly, three different cooling patterns, e.g. air cooling, water quenching and intensive quenching are proposed to better understand the formation of inter/intra-granular κ-carbides and its influence on tensile properties and mechanical behavior. These results may provide theoretical supports for the κ-carbides-related alloy design and microstructural modification of ultra-high-strength medium Mn low density steels.

2. Experimental procedures

A 50 kg ingot with a composition of Fe-11Mn-10Al-1.25C was prepared by induction melting. According to the Archimedes principle, the density of the present steel is measured as 6.81 g/cm^3 using a densitometry, which is about 13% lower than the pure Fe.

The ingot was heated at 1200 °C for 2 h and then hot forged into a slab with sectional dimension of 100 mm × 35 mm. After homogenization at 1200 °C for 2 h, the slab was hot rolled to the plates of 2 mm in thickness. Subsequently, the hot rolled plates were annealed at 1000 °C for 20 min and cooled to room temperature, following three different cooling patterns, e.g. air cooling, water quenching and intensive quenching (quenching in a 10% $CaCl_2$ solution for 1 s, followed by liquid nitrogen for 30 s), as schematically illustrated in Fig. 1. These samples cooled down by the above three styles are referred to as AC, WQ and IQ for convenience, respectively.

Tensile specimens of 6 mm width and gage length of 25 mm were machined from the annealed plates parallel to the rolling direction, according to the ASTM E8/E8M sub-size standard [15]. Tensile tests were carried out on a universal testing machine (SANSCMT5000) at an initial strain rate of 1×10^{-3} s^{-1} at room temperature. Interrupted tensile tests were performed as well at predetermined strains to examine the microstructural evolution and deformation mechanism at different strain stages.

Microstructural examination was carried out using an optical microscope (OM, OLYMPUS DSX500), scanning electron microscopy (SEM, Zeiss Ultra Plus) and transmission electron microscope (TEM, Tecnai G^2 20). Specimens for OM and SEM observations were electrolytic polished and then etched by a solution of 1 ml hydrochloric acid, 100 ml methanol and 4 g picric acid. Four representative optical micrographs (1194 × 1194 pixel) were used for each sample to measure the fraction of ferrite, based on the pixel method by the image analysis software (Image Pro Plus 6.0).

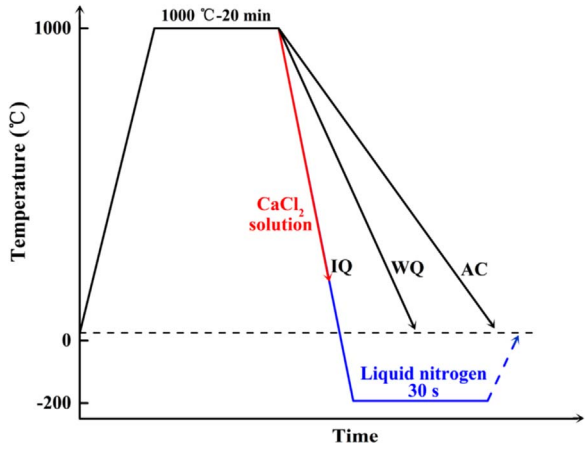

Fig. 1. Schematic illustration of three cooling procedures after solution-treatment in a Fe-11Mn-10Al-1.25C steel. AC: air cooling, WQ: water quench, IQ: intensive quench.

Thin foils for TEM observation were electro-polished by a twin-jet polisher using a mixed solution of 95% acetic acid and 5% perchloric acid. TEM analysis was performed at an acceleration voltage of 200 kV. Phase constituents were identified by X-ray diffraction (XRD, Rigaku, D/Max2250/PC) with Cu-Kα radiation (λ = 1.5405 Å). The samples were scanned in the angle range of 40–100° with a speed of 2°/min.

3. Results

3.1. Microstructures

Fig. 2 presents the optical micrographs of AC, WQ and IQ samples, demonstrating the notable difference in precipitation behavior with varying cooling patterns. In the AC sample, the precipitates are mainly distributed along the austenite grain boundaries (Fig. 2**(a)**). In the case of WQ, the chain-like ferrite and κ-carbide particles are dispersedly distributed in the austenitic matrix (Fig. 2**(b)**). In contrast, the IQ sample exhibits an almost fully austenitic structure with relatively coarse grains and some amount of annealing twins (Fig. 2**(c)**).

Fig. 3 shows the X-ray diffraction patterns of AC, WQ and IQ samples, indicating the presence of both the face/body-centered cubic (fcc/bcc) peaks for all experimental samples. The peaks of κ-carbides including (111) and (200) are detectable only in the WQ sample, which is probably due to the smaller fraction of the ordered nano-sized κ-carbides in both AC and IQ samples. The presence of κ-carbides in the AC sample can be proven by the broadening austenitic peaks [16]. The formation of κ-carbides with relatively larger lattice parameters is considered to be associated with spinodal decomposition, accompanied by the existence of the surrounding carbon-depleted austenite [3,13,16]. The observable X-ray sidebands in both WQ and IQ samples in Fig. 3 imply the sideband modulated structure composed of the disordered fcc austenite phase and $L'1_2$ ordered κ-carbide [13].

Fig. 4**(a)** shows the SEM morphologies of two different types of precipitates in the austenite matrix of AC sample. One type is the thin film κ-carbides, which are distributed continuously along the austenite grain boundaries. The other one is the blocky ferrite, which appears to be the distinct dark grains. In contrast, the WQ sample exhibits the relatively coarse κ-carbide particles with an average size of 0.6–2.6 μm, which are mainly located in the grain boundaries (Fig. 4**(b)**); only a few isolated ferrite particles are observed in the austenite matrix of IQ sample (Fig. 4**(c)**).

Fig. 5 shows the dark-field TEM morphologies of AC, WQ and IQ samples. Analysis of selected-area diffraction patterns (SAPDs) indicates that the particles among the austenitic matrix are κ-carbide precipitates. In the AC sample, the shape of κ-carbides is close to cuboidal, with its size ranging from 20 to 45 nm, see Fig. 5**(a)**. In comparison, both WQ and IQ samples exhibit very fine κ-carbide particles with an average size of less than 13 nm (Fig. 5**(b)** and **(c)**). It is also interesting to note that the intensity of the superlattice reflections in the AC sample is much higher than those of the other two samples.

3.2. Mechanical properties

Fig. 6**(a)** represents the engineering stress-strain curves of AC, WQ and IQ samples, and the corresponding tensile properties are summarized in Table 1. All tensile samples exhibit relatively high yield and ultimate tensile strengths (YS/UTS) of more than 1 GPa. Especially, both YS and UTS values of AC sample reach as high as 1.14 GPa and 1.21 GPa, respectively, but the total elongation to fracture (El) is quite low, only ~ 5%. As the cooling pattern changes from AC to WQ, the YS and UTS drop by 80–100 MPa, while the El value doubles. It is worth noting that the IQ sample exhibits similar YS and UTS values to the WQ with the significantly enhanced ductility of ~ 29.3%. Meanwhile, the